Lithium Cations Tightly Bound to Polychalcogenides: Synthesis and Solid-State Structures of $Li_2S_6(teeda)_2$, $Li_2S_4(pmdeta)_2$, and $Li_2Se_5(pmdeta)_2$

Kazuyuki Tatsumi,*,† Hiroyuki Kawaguchi,† Koji Inoue,† Kazuhide Tani,† and Roger E. Cramer*,‡

Departments of Chemistry, Faculty of Engineering Science, Osaka University, Toyonaka, Osaka 560, Japan, and University of Hawaii at Manoa, Honolulu, Hawaii 96822

Received October 1, 1992

Addition of *N,N,N',N'*-tetraethylethylenediamine (teeda) and *N,N,N',N'',N'''*-pentamethyldiethylenetriamine (pmdeta) to a toluene suspension of Li_2S_2 resulted in a homogeneous orange-red solution, from which we isolated $Li_2S_6(teeda)_2$ (**2**) and $Li_2S_4(pmdeta)_2$ (**3**), respectively. The selenide analog of **3**, $Li_2Se_5(pmdeta)_2$ (**4**), has been obtained from a reddish-brown toluene solution containing Li_2Se_2 and pmdeta, while a similar treatment of Li_2Se_2 and *N,N,N',N'*-tetramethylethylenediamine (tmeda) yielded $Li_2Se_4(tmeda)_2$ (**5**). In contrast, the Li_2Se_2/teeda system deposited lithium metal as particles or as a mirror. The lithium chalcogenides **2–4** have been characterized by X-ray structure determinations. Crystal data: **2**, monoclinic space group $P2_1$, a = 9.862(4) Å, b = 17.337(7) Å, c = 10.243(6) Å, β = 115.83(4)°, Z = 2, R = 0.057, and R_w = 0.083 for 2928 independent reflections; **3**, monoclinic space group $P2_1/c$, a = 14.04(1) Å, b = 14.23(1) Å, c = 16.007(7) Å, β = 111.08(5)°, Z = 4, R = 0.054, and R_w = 0.058 for 2171 independent reflections with $I > 3.0\sigma(I)$; **4**, triclinic space group $P\bar{1}$, a = 9.808(7) Å, b = 18.227(3) Å, c = 8.7930(6) Å, α = 98.092(9)°, β = 90.13(2)°, γ = 90.72(4)°, Z = 2, R = 0.044, and R_w = 0.055 for 3634 independent reflections with $I > 3.0\sigma(I)$. These crystals all consist of discrete molecular units, in which lithium ions are tightly bound to terminal chalcogen atoms. No strong intermolecular interactions were noticed. Molecule **2** has an intriguing bicyclic Li_2S_6 geometry, while the S_4^{2-} unit in **3** and the Se_5^{2-} unit in **4** exhibit zigzag chain structures. The Raman spectra of **2** and **3** and the ^1H NMR spectra of **2–4** are discussed.

Introduction

The polysulfides and polyselenides of the alkali and alkaline-earth metals have been known for sometime,[1] and a good number of crystal structures have appeared. However, characterization of lithium polychalcogenides is still limited, probably due to their propensity to decompose in water and in alcoholic solvents. The only well-characterized example so far is $Li_2S_6(tmeda)_2$ (**1**) (tmeda = *N,N,N',N'*-tetramethylethylenediamine), which was independently reported by us[2] and by a British group.[3] A key to that synthesis is addition of a suitable Lewis base, tmeda, which solubilizes lithium salts in water-free organic solvents, typically toluene. Interestingly the crystal structure of **1** was found to consist of discrete "molecular" units, in which two lithium cations bridge the terminal sulfurs of S_6^{2-} forming an unusual bicyclic Li_2S_6 unit. The lithiums are further coordinated by tmeda molecules completing a tetrahedral coordination sphere.

Now we extend our study of lithium polysulfides to those containing teeda (*N,N,N',N'*-tetraethylethylenediamine) and pmdeta (*N,N,N',N'',N'''*-pentamethyldiethylenetriamine). In the case of transition metal polysulfides, the size and geometry of metal–polysulfide rings vary dramatically depending on the metal and the auxiliary ligands. For instance, the $(C_5H_5)_2Ti$ moiety forms exclusively the six-membered TiS_5 ring with a chair conformation regardless of the nature of polysulfide reagents used,[4] while the sterically encumbered $(C_5Me_5)_2Ti$ moiety opts for the TiS_3 ring.[5] On the other hand, the $(C_5H_5)_2Mo$ and $(C_5H_5)_2W$ fragments tend to generate five-membered MS_4 rings.[6] Thus, we thought that use of the bulkier teeda ligand, instead of tmeda, might alter the coordination structure of **1** and that replacement of the bidentate $(N)_2$ chelates by the tridentate $(N)_3$ donor of pmdeta might alter the lithium–polysulfide bonding. We have also extended our study to the analogous, and yet structurally unknown, lithium polyselenide system. This paper reports the synthesis of these new lithium chalcogenides and the crystal structures of $Li_2S_6(teeda)_2$ (**2**), $Li_2S_4(pmdeta)_2$ (**3**), and $Li_2Se_5(pmdeta)_2$ (**4**).

Experimental Section

All experiments were carried out under an argon atmosphere using standard Schlenk techniques. Reagent-grade benzene, toluene, and THF were distilled from benzophenone ketyl under argon. The amines, teeda and pmdeda, and deuterated benzene and toluene were dried before use by trap-to-trap distillation from calcium hydride or sodium.

^1H NMR spectra were recorded on JEOL FX-90, JEOL GSX-270, and JEOL GSX-400 spectrometers. NMR data are listed in ppm downfield from TMS, while coupling constants are quoted in hertz. Raman spectra were measured on a JASCO R-800 spectrometer equipped with a He–Ne laser, where the crystal samples were sealed under Ar in thin-walled glass capillaries.

Lithium sulfides (Li_2S_2) and lithium selenides (Li_2Se_2) were made via stoichiometric reaction of lithium metal with elemental sulfur or elemental selenium in liquid ammonia.[7] The liquid ammonia was then evaporated under a flux of argon, to give light yellow (Li_2S_2) or reddish brown (Li_2Se_2) powders. Analogously, Li_2S_x (x = 4–6) compounds were prepared

† Osaka University.
‡ University of Hawaii.

(1) (a) Cotton, F. A.; Wilkinson, G. *Advanced Inorganic Chemistry*, 4th ed.; Wiley: New York, 1980; p 512. (b) Cusick, J.; Dance, I. *Polyhedron* **1991**, *10*, 2629 and references therein.
(2) Tatsumi, K.; Inoue, Y.; Nakamura, A.; Cramer, R. E.; VanDoorne, W.; Gilje, J. *Angew. Chem., Int. Ed. Engl.* **1990**, *29*, 422.
(3) Banister, A. J.; Barr, D.; Brooker, A. T.; Clegg, W.; Cunnington, M. C.; Doyle, M. J.; Drake, S. R.; Gill, W. R.; Manning, K.; Raithby, P. R.; Snaith, R.; Wade, K.; Wright, D. S. *J. Chem. Soc., Chem. Commun.* **1990**, 105.
(4) Shaver, A.; McCall, J. M. *Organometallics* **1984**, *3*, 1823–1829 and references therein.
(5) Bird, P. H.; McCall, J. M.; Shaver, A.; Siriwardane, U. *Angew. Chem., Int. Ed. Engl.* **1982**, *21*, 384.
(6) (a) Block, H. D.; Allman, R. *Cryst. Struct. Commun.* **1975**, *4*, 53. (b) Davis, B. R.; Bernal, I.; Köpf, H. *Angew. Chem., Int. Ed. Engl.* **1971**, *10*, 921.
(7) This Li_2S_2 sample gives Raman spectra nearly identical to those of Li_2S_2 prepared from the reaction between $LiEt_3BH$ (Super Hydride) and S_8 and is probably admixed with small quantities of other forms of lithium sulfides, e.g., Li_2S, Li_2S_3, and Li_2S_4 etc., as well as S_8. Disproportionation might take place in THF. In view of the dark color of the THF solution, the sulfur content of the solid obtained from the THF solution is probably higher than the original Li_2S_2 stoichiometry. The selenium content of the THF soluble portion of Li_2Se_2 could also be higher.

0020-1669/93/1332-4317$04.00/0

as orange powders from $1:x/16$ Li/S_8 reaction systems. Li_2S_2 and Li_2Se_2 are partly dissolved in THF. For the synthesis of **2–5**, either the THF soluble portion of Li_2E_2 (E = S, Se) or the solids obtained from the THF filtrates can be used. The elemental analysis was performed by sealing the crystalline samples in thin aluminum tubes. The analytical data fit reasonably to the formulas derived from the X-ray study.

Preparation of Li_2S_6(teeda)$_2$ (2). Li_2S_2 (2.1 g, 27 mmol) was washed three times with THF (3 × 30 mL), and the brown-red THF filtrate was evaporated in vacuo, leaving a yellow solid. Excess teeda (3.4 mL, 16 mmol) was added to a suspension of this yellow solid in toluene (60 mL), to give a homogeneous orange-red solution. After a small amount of insoluble material was filtered off, the solution was concentrated to ca. 30 mL and refrigerated overnight at −20 °C, yielding 1.4 g (2.5 mmol, 9.2% yield based on Li) of orange crystals of **2**. Mp: 85–88 °C. ^{1}H NMR (90 MHz, C_6D_6, room temperature): δ (ppm) 1.02 (t, J_{HH} = 7, 24H, NCH_2CH_3), 2.36 (s, 8H, NCH_2CH_2N), 2.66 (q, J_{HH} = 7, 16H, NCH_2CH_3). Raman (crystals) (cm^{-1}): 498 w, 466 s, 405 s, 248 w, 235 w, 204 s. Anal. Calcd for $C_{20}H_{48}N_4Li_2S_6$: C, 43.60; H, 8.78; N, 10.17; S, 34.92. Found: C, 42.55; H, 8.38; N, 10.47; S, 34.75.

Preparation of Li_2S_4(pmdeta)$_2$ (3). The preparation of the pmdeta compound was similar to that of **2**. Addition of pmdeta (3.1 mL, 15 mmol) in toluene to the yellow solid obtained from the THF filtrate of Li_2S_2 (1.5 g, 19 mmol) gave a green solution, from which 0.20 g of **3** (0.41 mmol, 2% yield based on Li) was isolated as orange needles. We also attempted a direct reaction of pmdeta with Li_2S_4 in toluene. Thus, pmdeta (3.8 mL, 18 mmol) was added to a toluene suspension (70 mL) of Li_2S_4 (1.2 g, 8.4 mmol) and stirred for 2 h. The resulting green solution was filtered, and upon standing overnight at −20 °C orange needles of **3** (1.7 g, 3.4 mmol, 41% yield) were obtained. Mp: 126–128 °C dec. ^{1}H NMR (270 MHz, C_6D_6, room temperature): δ (ppm) 2.08 (s, 16H, NCH_2CH_2N), 2.29 (s, 6H, $NCH_2CH_2N(CH_3)CH_2CH_2N$), 2.38 (s, 24H, $N(CH_3)_2$). Raman (crystals) (cm^{-1}): 505 w, 440 m, 403 s, 256 w, 121 m. Anal. Calcd for $C_{18}H_{46}N_6Li_2S_4$: C, 44.23; H, 9.49; N, 17.19; S, 26.24. Found: C, 44.11; H, 9.16; N, 16.78; S, 27.53.

Preparation of Li_2Se_5(pmdeta)$_2$ (4). The selenide compound **4** was prepared in an analogous manner. Reddish brown Li_2Se_2 (3.7 g, 22 mmol) prepared in liquid ammonia was washed three times with THF (30 mL × 3), and the dark-red THF filtrate was evaporated in vacuo to give a dark-red solid. Addition of pmdeta (8 mL, 29 mmol) to a suspension of this solid in toluene led to a dark-red solution, from which **4** (1.8 g, 2.4 mmol, 11% yield) was obtained as brown needles. ^{1}H NMR (270 MHz, C_6D_6, room temperature): δ (ppm) 1.97 (s, br, 16H, NCH_2CH_2N), 2.28 (s, 6H, $NCH_2CH_2N(CH_3)CH_2CH_2N$), 2.39 (s, 24H, $N(CH_3)_2$). Anal. Calcd for $C_{18}H_{46}N_6Li_2Se_5$: C, 28.62; H, 6.14; N, 11.13. Found: C, 28.64; H, 6.00; N, 11.02.

Preparation of Li_2Se_4(tmeda)$_2$ (5). Addition of tmeda (3 mL, 20 mmol) to a toluene suspension of the dark-red solid obtained from the THF-soluble portion of Li_2Se_2 (2.3 g, 13 mmol) resulted in a homogeneous dark-red solution. Upon cooling of the solution to ambient temperature, compound **5** (1.8 g, 2.5 mmol) was isolated as brown plates. ^{1}H NMR (100 MHz, C_6D_6, room temperature): δ (ppm) 1.95 (s, 12H, $N(CH_3)$), 2.26 (s, 4H, NCH_2CH_2N). Anal. Calcd for $C_{12}H_{32}N_4Li_2Se_4$: C, 25.64; H, 5.74; N, 9.97. Found: C, 24.43; H, 5.29; N, 9.48.

Treatment of "Li_2Se_2" with teeda. The dark-red solid obtained from the THF filtrate of Li_2Se_2 (3.7 g, 22 mmol) was added to 40 mL of toluene. Then teeda (3.0 mL, 14 mmol) was added to the resulting suspension with stirring. At first the suspension became a dark-red homogeneous solution, and then in a few seconds, lustrous particles were formed along with a dark-brown powder. After filtration, the dark-red solution was concentrated and kept overnight. A metallic mirror was deposited on the inner surface of the vessel, and at the same time a dark-brown crystalline powder precipitated. The metallic particles and the mirror were found to be lithium. Formation of a lithium mirror was also noticed, when the aforementioned metallic particles and dark brown crystalline powder were redissolved in teeda (excess)/toluene and allowed to stand overnight.

X-ray Crystallographic Study of 2. An orange, platelike crystal of **2** (0.9 × 0.7 × 0.13 mm) was sealed in a thin-walled glass capillary under argon. The unit cell determination and data collection were carried out on a Siemens R3 diffractometer system at the University of Hawaii. Crystal quality and unit cell parameters, which were determined from the carefully determined locations of 24 reflections with 2θ values between 15.21 and 27.37°, were verified by axial photographs. The unit cell was monoclinic, and the systematic absence implied the space group $P2_1$ or $P2_1/m$. Given the puckered teeda and S_6 rings in the molecule, mirror symmetry would require disorder, so space group $P2_1$ was the likely choice.

Table I. Crystal Data for Li_2S_6(teeda)$_2$ (**2**), Li_2S_4(pmdeta)$_2$ (**3**), and Li_2Se_4(pmdeta)$_2$ (**4**)

	2	**3**	**4**
formula	$C_{20}H_{48}Li_2N_4S_6$	$C_{18}H_{46}Li_2N_6S_4$	$C_{18}H_{46}Li_2N_6Se_5$
fw	550.9	488.7	755.3
space group	$P2_1$	$P2_1/c$	$P\bar{1}$
a, Å	9.862(4)	14.04(1)	9.808(7)
b, Å	17.337(7)	14.23(1)	18.227(3)
c, Å	10.243(6)	16.007(7)	8.7930(6)
α, deg	90	90	98.092(9)
β, deg	115.83(4)	111.08(5)	90.13(2)
γ, deg	90	90	90.72(4)
V, Å^3	1576(1)	2985(4)	1556(1)
Z	2	4	2
ρ_{calcd}, g/cm^3	1.16	1.087	1.612
μ, cm^{-1}	4.31	3.20	58.41
radiation	Mo Kα	Mo Kα	Mo Kα
unique data	2928	2171($I > 3.0\sigma(I)$)	3634($I > 3.0\sigma(I)$)
data-to-param ratio	8.5:1	8.0:1	13.0:1
R (R_w)	0.057 (0.083)	0.054 (0.058)	0.044 (0.055)

A preliminary data set, collected at a fast scan rate and a 2θ limit of 35°, yielded 890 data with $F > 2\sigma(F)$, which were subjected to a SHELXTLPLUS direct methods structure solution attempt. The mean $E^2 - 1$ was in good agreement with an acentric unit cell, supporting the choice of $P2_1$ as the correct space group. This direct methods solution yielded the positions of six sulfur atoms. Upon least-squares refinement, the inner sulfur atoms S3 and S4 had large thermal parameters, and large peaks appeared near these positions in the Fourier map, suggesting that S3 and S4 were disordered. Including all heavy atoms as well as the partial sulfurs gave the R value of 0.1040. At this point we switched to a carefully collected data set, which included Friedel pairs. Refinement for all 2928 unique data gave $R = 0.1124$. After the data were corrected for absorption based on ψ scans of four reflections with 2θ values from 11.98 to 32.79°, the R value was lowered to 0.1119. The structure was inverted to determine the absolute configuration, yielding a higher R value of 0.1121. After anisotropic refinement for all atoms except Li, the disorder of the sulfur positions was addressed by removing S2–S5 and calculating a Fourier map, which revealed disorder for S2 and S5 as well as S3 and S4. Refinement of the sulfur occupancies led to 55.2(6)% for the sulfur A sites and 44.8(6)% for the sulfur B sites. Hydrogen atoms were then added, where the CH_2 hydrogens were allowed to ride on the attached carbon, while the methyls were refined as rigid groups. The final R values were $R = 0.0572$ and $R_w = 0.0826$, and the final difference Fourier map shows a maximum residual peak of 0.35 e/Å^3. Table I shows the crystal data and other relevant information.

X-ray Crystallographic Study of 3 and 4. Crystals of **3** (1.0 × 0.6 × 0.2 mm) and **4** (0.6 × 0.3 × 0.2 mm) were mounted in thin-walled glass capillaries under argon. The reflection data were collected by the ω–2θ scan technique on a Rigaku AFC5R diffractometer at Osaka University using graphite-monochromatized Mo Kα radiation (λ = 0.710 69 Å) and a 12-kW rotating anode generator. The unit cell dimensions of **3** were determined by a least-squares refinement of the setting angles of 15 centered reflections in the range $8.8 < 2\theta < 25.1°$, while for **4** 23 reflections in the range $20.9 < 2\theta < 25.1°$ were used. During the data collection to a maximum 2θ value of 50.1° (for **3**) or 55.1° (for **4**), three standard reflections were recorded after every 100 reflections, which showed no significant decay. An empirical absorption correction was applied with use of azimuthal scans of three reflections. The data were also corrected for Lorentz and polarization effects. In the case of **3**, the systematic absences point unambiguously to the space group $P2_1/c$ (No. 14). A summary of crystal data is provided in Table I.

The structure of **3** was solved by direct methods using the TEXSAN crystallographic software package of the Molecular Structure Corp., which clearly revealed the positions of four sulfur atoms. The remaining non-hydrogen atoms were found in succeeding difference Fourier syntheses. The structure was refined by a full-matrix least-squares refinement using 2171 reflections with $I > 3.0\sigma(I)$ out of the 5525 unique reflections. Anomalous dispersion effects for non-hydrogen atoms were included in F_c. All the non-hydrogen atoms were refined anisotropically and hydrogen atoms were put in calculated positions for the final cycle of the refinement. Refinement converged at $R = 0.054$ ($R_w = 0.058$), and the final difference Fourier map was essentially featureless with the largest peak being 0.32 e/Å^3.

The structure of **4** was also solved by direct methods. However from the MITHRIL routine, only three selenium positions were unambiguously determined, and the remaining selenium atoms as well as the other heavy

Table II. Fractional Atomic Coordinates and Equivalent Isotropic Thermal Parameters (Å²) of Non-Hydrogen Atoms in $Li_2S_6(teeda)_2$ (**2**) with Esd's in Parentheses

atom	x	y	z	U_{eq}
S1	0.4278(2)	0.5	0.0890(2)	0.0062(1)
S2A	0.535(2)	0.483(1)	0.310(2)	0.0091(5)
S2B	0.544(2)	0.471(2)	0.298(2)	0.0084(5)
S3A	0.4916(4)	0.5587(3)	0.4209(4)	0.0089(2)
S3B	0.4324(7)	0.5066(4)	0.4149(4)	0.0094(2)
S4A	0.2683(4)	0.5522(3)	0.3846(3)	0.0091(2)
S4B	0.4085(6)	0.6250(3)	0.4117(4)	0.0095(2)
S5A	0.177(1)	0.6523(7)	0.2783(9)	0.0072(4)
S5B	0.173(2)	0.643(1)	0.272(2)	0.0117(8)
S6	0.1404(2)	0.6421(1)	0.0663(2)	0.0064(1)
N1	0.0199(5)	0.4582(3)	-0.1917(5)	0.0061(2)
N2	0.0562(5)	0.4022(3)	0.0929(5)	0.0064(2)
N3	0.5500(6)	0.7422(3)	0.1969(7)	0.0082(3)
N4	0.3946(6)	0.7001(3)	-0.1173(6)	0.0074(3)
C1	0.0046(7)	0.3775(4)	-0.1603(7)	0.0073(3)
C2	-0.0473(8)	0.3662(4)	-0.0448(7)	0.0079(3)
C3	0.1135(8)	0.4663(5)	-0.2712(8)	0.0088(3)
C4	0.051(1)	0.4331(7)	-0.4237(8)	0.0127(6)
C5	-0.1306(7)	0.4931(4)	-0.2732(8)	0.0084(3)
C6	-0.1271(9)	0.5768(5)	-0.3039(9)	0.0094(4)
C7	0.1913(7)	0.3557(4)	0.1746(8)	0.0081(3)
C8	0.1733(9)	0.2773(5)	0.231(1)	0.0101(4)
C9	-0.0179(9)	0.4179(6)	0.1846(9)	0.0100(4)
C10	-0.131(1)	0.4823(6)	0.128(1)	0.0122(6)
C11	0.569(1)	0.7845(6)	0.082(1)	0.0121(6)
C12	0.448(1)	0.7794(6)	-0.057(1)	0.0125(5)
C13	0.4575(9)	0.7870(5)	0.256(1)	0.0119(5)
C14	0.518(1)	0.8616(9)	0.324(2)	0.022(1)
C15	0.6980(9)	0.7220(6)	0.319(1)	0.0111(5)
C16	0.779(1)	0.6604(6)	0.295(1)	0.0119(5)
C17	0.2418(9)	0.7020(5)	-0.2241(8)	0.0090(4)
C18	0.202(1)	0.7501(7)	-0.360(1)	0.0119(5)
C19	0.496(1)	0.6680(9)	-0.172(2)	0.0153(8)
C20	0.499(2)	0.5901(8)	-0.195(2)	0.020(1)
Li1	0.1460(9)	0.5005(6)	0.0306(9)	0.0055(2)
Li2	0.407(1)	0.6431(7)	0.079(1)	0.0064(2)

atoms were located in difference Fourier maps. Full-matrix least-squares refinement using the 3634 observed reflections with $I > 3.0\sigma(I)$ out of the 6567 unique reflections converged at $R = 0.044$ ($R_w = 0.055$), where all non-hydrogen atoms were refined anisotropically and hydrogens were at calculated positions. A final difference Fourier map showed the maximum residual peak of 0.63 e/Å³.

The resulting atomic positional parameters of the non-hydrogen atoms for **2**–**4** are listed in Tables II–IV, respectively, along with the equivalent isotropic thermal parameters, $U(eq)$ or $B(eq)$. Additional crystallographic data are available as supplementary material.

Results and Discussion

A series of new lithium chalcogenides were synthesized by a method analogous to that used for preparation of $Li_2S_6(tmeda)_2$.[2] A toluene slurry of a yellow solid obtained from the THF-soluble portion of Li_2S_2 becomes homogeneous orange-red and green solutions upon addition of teeda and pmdeta, respectively. From such solutions we were able to isolate $Li_2S_6(teeda)_2$ (**2**) or $Li_2S_4(pmdeta)_2$ (**3**) as orange crystals. The isolated yields are low (2–9%), because we used the "THF-soluble" portion of Li_2S_2, and the yields were calculated on the basis of total Li_2S_2. If teeda or pmdeta is added directly to a toluene slurry of Li_2S_2, the yield of **2** or **3** increases to 30–40%, but this method occasionally gives a small quantity of S_8 crystals as a side product. Interestingly regardless of the composition of the starting lithium sulfides, Li_2S_x (x = 2–6), the crystals isolated are **2** and **3**.

Following the successful isolation of the polyamine adducts of lithium polysulfides, we carried out a synthesis of the analogous lithium selenides. When pmdeta was added to a dark brown solid, made from the THF-soluble portion of Li_2Se_2, suspended in toluene, the suspension immediately became a clear dark-red solution, from which brown crystals of $Li_2Se_5(pmdeta)_2$ (**4**) were deposited. A similar treatment with tmeda also afforded thin dark-red plates formulated as $Li_2Se_4(tmeda)_2$ (**5**), but X-ray-quality crystals did not grow. As the ^1H NMR spectrum of these crystals dissolved in C_6D_6 closely resembles that of **1**, the product is likely to assume a bicyclic structure analogous to **1** and **2**.

In the case of the Li_2Se_2/teeda system, the situation is very different. A toluene suspension of a dark brown THF-soluble solid became first a dark-red homogeneous solution upon addition

Table III. Fractional Atomic Coordinates and Equivalent Isotropic Thermal Parameters (Å²) of Non-Hydrogen Atoms in $Li_2S_4(pmdeta)_2$ (**3**) with Esd's in Parentheses

atom	x	y	z	B_{eq}
S1	0.6605(1)	0.5536(1)	0.2517(2)	7.6(1)
S2	0.7191(1)	0.4317(1)	0.3212(1)	6.7(1)
S3	0.8520(1)	0.3975(1)	0.3021(1)	5.62(8)
S4	0.8193(1)	0.3088(1)	0.1947(1)	5.84(8)
N1	0.9264(4)	0.6492(4)	0.3792(3)	5.7(3)
N2	0.8154(4)	0.7470(4)	0.2141(4)	5.6(3)
N3	0.8859(4)	0.5868(3)	0.1457(3)	5.0(3)
N4	0.5146(4)	0.3013(4)	0.1317(4)	5.6(3)
N5	0.6179(4)	0.1276(4)	0.1313(4)	5.9(3)
N6	0.6898(4)	0.1647(4)	0.3235(4)	5.7(3)
C1	0.9068(8)	0.7506(6)	0.3744(6)	10.2(6)
C2	0.8933(7)	0.7915(5)	0.2896(7)	8.7(5)
C3	0.8420(6)	0.7538(5)	0.1343(6)	8.8(5)
C4	0.9138(7)	0.6811(5)	0.1287(5)	8.3(5)
C5	1.0336(6)	0.6283(6)	0.3963(5)	9.0(5)
C6	0.8989(6)	0.6070(6)	0.4516(5)	8.6(4)
C7	0.7134(6)	0.7866(6)	0.1952(6)	10.2(5)
C8	0.7999(6)	0.5493(6)	0.0727(5)	8.2(4)
C9	0.9743(6)	0.5247(5)	0.1610(5)	8.5(5)
C10	0.4578(5)	0.2167(6)	0.0923(6)	8.6(4)
C11	0.5177(7)	0.1489(6)	0.0628(5)	8.4(4)
C12	0.6088(6)	0.0602(5)	0.1955(6)	7.2(4)
C13	0.6902(6)	0.0722(5)	0.2841(6)	7.9(4)
C14	0.4576(5)	0.3513(6)	0.1772(6)	9.2(5)
C15	0.5294(5)	0.3649(6)	0.0667(5)	8.4(4)
C16	0.6877(6)	0.0948(5)	0.0882(6)	9.3(5)
C17	0.7873(6)	0.1825(6)	0.3931(5)	9.2(4)
C18	0.6106(7)	0.1680(6)	0.3611(6)	10.5(5)
Li1	0.8285(7)	0.5997(7)	0.2533(6)	4.4(4)
Li2	0.6642(7)	0.2538(7)	0.2110(7)	5.1(5)

Table IV. Fractional Atomic Coordinates and Equivalent Isotropic Thermal Parameters (Å²) of Non-Hydrogen Atoms in $Li_2Se_5(pmdeta)_2$ (**4**) with Esd's in Parentheses

atom	x	y	z	B_{eq}
Se1	0.2646(1)	0.08108(5)	0.1968(1)	4.96(4)
Se2	0.13624(9)	0.18447(5)	0.2769(1)	4.87(4)
Se3	0.2865(1)	0.28189(5)	0.3752(1)	4.76(4)
Se4	0.26243(9)	0.38109(5)	0.2370(1)	4.47(4)
Se5	0.10914(8)	0.46514(5)	0.3629(1)	4.30(4)
N1	0.3888(7)	0.1692(4)	-0.1716(8)	4.9(4)
N2	0.1113(7)	0.1187(5)	-0.2128(8)	5.3(4)
N3	0.2780(7)	-0.0161(4)	-0.2351(8)	5.0(4)
N4	-0.2619(7)	0.5130(4)	0.2215(7)	4.2(3)
N5	-0.2064(8)	0.3587(4)	0.1259(8)	5.1(4)
N6	-0.2303(7)	0.3450(4)	0.4465(8)	4.5(3)
C1	0.398(1)	0.2293(7)	-0.045(1)	8.2(7)
C2	0.529(1)	0.1524(7)	-0.231(2)	9.8(8)
C3	0.311(1)	0.1891(6)	-0.299(1)	7.7(7)
C4	0.155(1)	0.1875(6)	-0.262(1)	7.5(6)
C5	-0.019(1)	0.1283(7)	-0.131(1)	8.4(7)
C6	0.097(1)	0.0576(6)	-0.342(1)	6.6(5)
C7	0.136(1)	-0.0166(7)	-0.285(1)	8.6(7)
C8	0.298(1)	-0.0767(6)	-0.140(1)	9.0(7)
C9	0.367(1)	-0.0295(8)	-0.367(1)	9.9(8)
C10	-0.181(1)	0.5789(6)	0.216(1)	6.6(6)
C11	-0.390(1)	0.5332(6)	0.297(1)	6.9(6)
C12	-0.281(1)	0.4742(6)	0.059(1)	7.2(6)
C13	-0.309(1)	0.3993(7)	0.049(1)	7.2(6)
C14	-0.089(1)	0.3389(7)	0.034(1)	8.7(7)
C15	-0.269(2)	0.2960(8)	0.178(2)	12(1)
C16	-0.265(2)	0.2871(8)	0.326(2)	14(1)
C17	-0.126(1)	0.3204(7)	0.547(1)	8.3(7)
C18	-0.350(1)	0.3648(6)	0.535(1)	6.7(5)
Li1	0.277(1)	0.0875(8)	-0.092(2)	4.7(7)
Li2	-0.152(1)	0.4333(7)	0.331(1)	3.7(6)

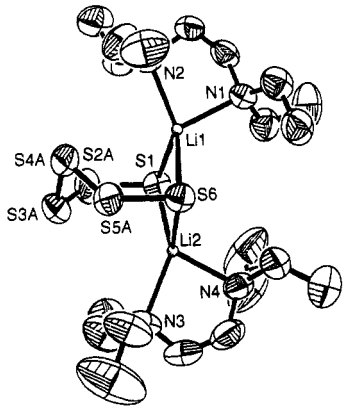

Figure 1. Structure and labeling scheme for $Li_2S_6(teeda)_2$ (**2**), where only one of the two sets of disordered atoms, i.e., S2A–S5A (55.2% occupancy), is included. The thermal ellipsoids are drawn at the 50% probability level.

Table V. Selected Bond Distances (Å) and Bond Angles (deg) for $Li_2S_6(teeda)_2$ (**2**) with Esd's in Parentheses

S1–S2A	2.06(2)	S5B–S6	1.99(2)
S1–S2B	2.00(2)	Li1–S1	2.575(9)
S2A–S3A	1.90(2)	Li1–S6	2.49(1)
S2B–S3B	2.04(3)	Li2–S1	2.49(1)
S3A–S4A	2.071(6)	Li2–S6	2.57(1)
S3B–S4B	2.065(8)	Li1–N1	2.191(9)
S4A–S5A	2.04(1)	Li1–N2	2.14(2)
S4B–S5B	2.16(2)	Li2–N3	2.22(1)
S5A–S6	2.05(1)	Li2–N4	2.20(1)
Li1–S1–S2A	103.9(6)	S1–Li1–S6	93.4(3)
Li1–S1–S2B	107.7(6)	S1–Li2–S6	93.5(4)
S1–S2A–S3A	114.7(9)	S1–Li1–N1	107.8(4)
S2A–S3A–S4A	110.8(5)	S1–Li1–N2	118.2(4)
S3A–S4A–S5A	103.8(4)	S6–Li1–N1	116.4(4)
S4A–S5A–S6	109.0(6)	S6–Li1–N2	134.7(5)
S1–S2B–S3B	110.5(9)	N1–Li1–N2	85.6(4)
S2B–S3B–S4B	112.1(8)	S1–Li2–N3	136.8(4)
S3B–S4B–S5B	103.6(6)	S1–Li2–N4	117.0(5)
S4B–S5B–S6	109(1)	S6–Li2–N3	115.3(5)
S5A–S6–Li1	103.6(4)	S6–Li2–N4	107.9(4)
S5B–S6–Li1	99.0(7)	N3–Li2–N4	85.2(5)

of teeda, and then, in a few seconds(!), lustrous particles were formed along with a dark-brown powder. When the remaining dark-red solution stood overnight, a metallic mirror was deposited on the inner surface of the vessel. These metallic products are lithium, and further study of this reaction is underway.

The amine adducts of lithium sulfides and lithium selenides described above are all highly hygroscopic and air-/moisture-sensitive. They dissolve readily in benzene, toluene, and THF, assuming orange (**1**, **2**), green (**3**), and dark red (**4**, **5**) colors but are hardly soluble in hexane. The DMF and CH_3CN solutions of **1**–**3** exhibit an intense blue color (absorption maximum at 615 nm), probably because the S_3^- anion radical is generated.[8] We think the green color of toluene solutions of **3** is also caused by the presence of a small amount of the S_3^- blue chromophore, for its UV/visible spectrum exhibits a weak band at ca. 610 nm.

Crystal Structure of 2. Single crystals of **2** are composed of discrete "molecular" units of $Li_2S_6(teeda)_2$, with no unusual short contacts between adjacent molecules. Figure 1 presents a perspective drawing of the molecule with the atom-labeling scheme. Of the disordered inner sulfurs, those of 55.2% occupancy (S2A–S5A) are shown. The selected bond distances and angles are listed in Table V.

The molecular structure consists of an S_6^{2-} chain in a horseshoe conformation, placing the terminal sulfurs in close proximity.

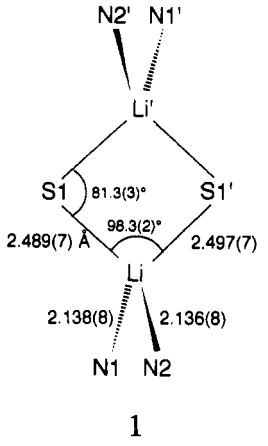

1

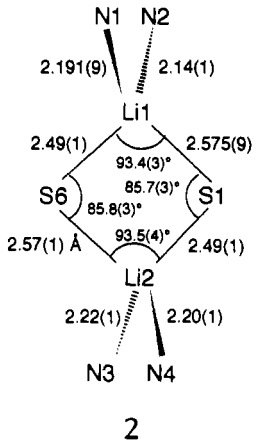

2

Figure 2. Comparison of bond distances and angles for the Li_2S_2 portions of $Li_2S_6(tmeda)_2$ (**1**) (left) and $Li_2S_6(teeda)_2$ (**2**) (right).

They chelate two lithium cations, one above the S_6^{2-} unit and the other below, resulting in a bicyclic Li_2S_6 geometry. Such a bicyclic form was found first in the structure of $Li_2S_6(tmeda)_2$ (**1**)[2,3] and it is unique among the alkali- and alkaline earth–polysulfides. This Li coordination also differs from the known structures of transition metal polysulfides.[9] The polysulfides in NaS_4,[10] $BaS_4(H_2O)$,[11] K_2S_5,[12] and Cs_2S_6[13] etc. are all ionic and acyclic, and the cations do not bind to specific sulfur atoms. In contrast, the Li–S interactions in **1** and **2** are sufficiently strong to hold together the two ends of the semicircular hexasulfide.

Although the molecule possesses no crystallographic symmetry, it does have approximate 2-fold symmetry, where the pseudo-2-fold axis passes through the midpoint of a line connecting the two terminal sulfurs, $(S1–S6)_{ct}$, and that of the two central sulfurs, $(S3A–S4A)_{ct}$ and $(S3B–S4B)_{ct}$. Due to the pseudosymmetry, the two Li(teeda) components are nearly isostructural. The Li1–S1–Li2–S6 quadrilateral is slightly folded, so that the dihedral angle between the two LiS_2 triangular faces is 166.0°. The corresponding Li_2S_2 quadrilateral of **1** is also folded but to a lesser extent (169.4°). Each teeda ligand is situated approximately perpendicular to the corresponding LiS_2 plane: the dihedral angle between the Li1–S1–S6 and Li1–N1–N2 planes is 90.3°, and the angle between the Li2–S1–S6 and Li2–N3–N4 planes is 91.9°. However, the LiS_2N_2 coordination spheres are highly distorted from an ideal tetrahedron, in such a way that the teeda units tilt away from S_6^{2-}; $N2–Li1–(S1–S6)_{ct}$ = 148.7° vs $N1–Li1–(S1–S6)_{ct}$ = 123.1°, and $N3–Li2–(S1–S6)_{ct}$ = 147.2° vs $N4–Li2–(S1–S6)_{ct}$ = 123.7°. This deformation can be rationalized in terms of the steric repulsion between the ethyl groups on teeda and the sulfide ring. In fact this distortion is larger for **2** than **1**.

Although the overall structure of **2** is closely related to that of **1**, there are some important differences in the metrical parameters associated with the Li coordination spheres as shown in Figure 2. Smaller S–Li–S angles and longer Li–N distances are observed for **2** compared to **1**. Again the steric bulk of teeda, relative to tmeda, must be responsible for the trends. The other obvious difference is that lithiums in **2** link the terminal sulfurs unsymmetrically as reflected in the long Li1–S1 and Li2–S6 distances, while for **1** the mode of lithium coordination is essentially symmetric. This results in a rhomboid-to-parallelogramic deformation of the Li_2S_2 quadrilateral upon going from **1** to **2**. The mean Li–S distance (2.530 Å) of **2** is at the long extreme of the known Li–S lengths in four-coordinate lithium complexes: [Li-

(8) (a) Bonnaterre, R.; Cauquis, G. *J. Chem. Soc., Chem. Commun.* **1972**, 293. (b) Gruen, D. M.; McBeth, R. L.; Zielen, A. J. *J. Am. Chem. Soc.* **1971**, *93*, 6691.

(9) Draganjac, M.; Rauchfuss, T. B. *Angew. Chem., Int. Ed. Engl.* **1985**, *24*, 742.

(10) Tegman, R. *Acta Crystallogr., Sect. B* **1973**, *B29*, 1463.

(11) Abrahams, S. C.; Bernstein, J. L. *Acta Crystallogr., Sect. B* **1969**, *B25*, 2365.

(12) Kelly, B.; Woodward, P. *J. Chem. Soc., Dalton Trans.* **1976**, 1314.

(13) Abrahams, S. C.; Grison, E. *Acta Crystallogr.* **1953**, *6*, 206.

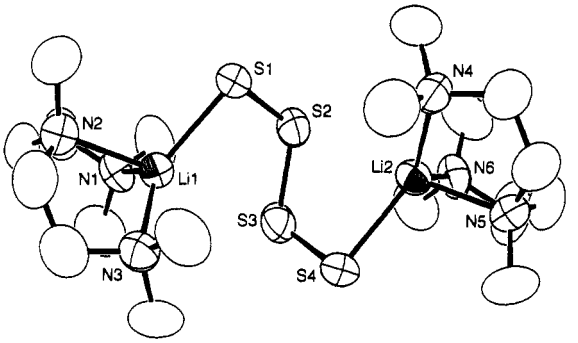

Figure 3. ORTEP drawing of $Li_2S_4(pmdeta)_2$ (**3**). Thermal ellipsoids represent the 50% probability surface.

Table VI. Selected Bond Distances (Å) and Bond Angles (deg) for $Li_2S_4(pmdeta)_2$ (**3**) with Esd's in Parentheses

S1–S2	2.067(3)	Li1–N2	2.18(1)
S2–S3	2.054(3)	Li1–N3	2.16(1)
S3–S4	2.048(3)	Li2–N4	2.14(1)
Li1–S1	2.438(9)	Li2–N5	2.16(1)
Li2–S4	2.42(1)	Li2–N6	2.13(1)
Li1–N1	2.11(1)		
Li1–S1–S2	91.4(2)	N1–Li1–N3	119.3(5)
S1–S2–S3	109.0(1)	N2–Li1–N3	82.5(4)
S2–S3–S4	109.3(1)	S4–Li2–N4	124.4(5)
S3–S4–Li2	92.7(3)	S4–Li2–N5	107.3(4)
S1–Li1–N1	113.2(4)	S4–Li2–N6	113.6(5)
S1–Li1–N2	105.9(4)	N4–Li2–N5	83.7(4)
S1–Li1–N3	127.3(4)	N4–Li2–N6	121.6(5)
N1–Li1–N2	84.9(4)	N5–Li2–N6	85.9(4)

$(tmeda)]_2[SCH_2CH_2CH_2SC(CH_3)]_2$,[14] 2.52 Å; $[Li(thf)]_4[(C_5Me_5)Ta(S)_3]_2$,[15] 2.44–2.54 Å; $[Li(dme)]_4[U(SCH_2CH_2S)_4]$,[16] 2.42 Å; polymeric-$CH_3SLi$, 2.4 Å.[17] While the disorder problem prevents us from making accurate comparisons between the outer and inner S–S bond lengths, the S–S distances are not very unusual.

Crystal Structure of 3. The solid-state structure of **3** is composed of well-separated molecular units of $Li_2S_4(pmdeta)_2$. The molecular structure is displayed in Figure 3 with the atom-numbering scheme, and the bond distances and angles are given in Table VI. Unlike **1** and **2**, no disorder occurs at the sulfur positions.

In contrast to the bicyclic Li_2S_6 structures of **1** and **2**, the molecule **3** contains a zigzag tetrasulfide chain. The S_4^{2-} chain is bound by lithium cations at each end, and the tridentate pmdeta ligand completes coordination at each lithium. The tridentate nature of the pmdeta chelate and the concomitant steric crowding around Li, caused by the five methyl groups, allow the lithium cation to interact strongly with only a single sulfur atom. As Figure 2 indicates, the pmdeta ligand covers up a good part of the Li coordination sphere. Although acyclic forms of S_x^{2-} dianions are common in the structures of alkali- and alkaline earth–polysulfides,[10-13] tight coordination of alkali metal ions to polysulfide chains is unprecedented. The mean Li–S distance of 2.432 Å falls in the normal range[14-17] but is clearly shorter than those of **1** and **2**.

The S_4^{2-} chain is skewed with the torsional angle of 92.1(1)°, which is similar to the one observed for the discrete S_4^{2-} unit in Na_2S_4 (97.81). Also the mean S–S–S angle of 109.2(1)° resembles closely that of Na_2S_4 (109.76(2)°). Thus, the strong Li–S interactions found in **3** do not influence the angular parameters of S_4^{2-}. There is not a clear trend in the S–S bond distances. For dialkyl tetrasulfides the terminal S–S bonds are shorter than the central S–S bond.[18] Conversely, chelation of S_4^{2-} to early transition metals tends to give a notably longer terminal S–S bond length (>0.10 Å, $(C_5H_5)_2MoS_4$ and $(C_5H_5)_2WS_4$)[6] presumably due to M–S π interactions, while the difference is reduced for late transition metals such as $(Ph_3P)_2PtS_4$,[19] $(Et_4N)_2Ni(S_4)_2$, and $(Et_4N)_2Zn(S_4)_2$.[20] In the case of unligated S_4^{2-} chains, it remains a matter of debate whether or not terminal bonds should be shorter than central bonds.[10,11] The S–S bond lengths may be sensitive to weak interactions of the sulfurs with countercations and/or to crystal packing forces.

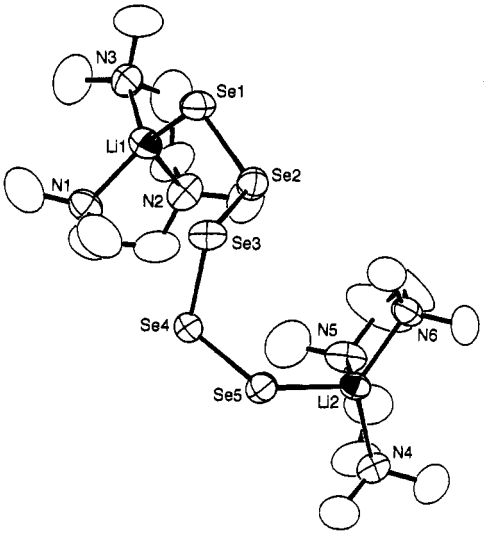

Figure 4. ORTEP drawing of $Li_2Se_5(pmdeta)_2$ (**4**). Thermal ellipsoids represent the 50% probability surface.

Each Li–S bond orients approximately cis to the inner S2–S3 bond. This cisoid Li–S–S–S configuration is reflected by the relatively small torsional angles of 23.2(2) and 24.6(3)°. Also the mean Li–S–S angle (91.6°) is substantially smaller than the tetrahedral angle and is even smaller than that of **2** (103.8°). Furthermore, the N1–Li1–N3 and N4–Li2–N6 angles are larger by 39–36° than the other N–Li–N bite angles, while the Li1, N1, N3, and S1 atoms are nearly coplanar (maximum deviation, 0.03 Å) and so are the Li2, N4, N6, and S4 atoms (maximum deviation, 0.06 Å). From these observations one might think that there is some attractive force between lithium and the inner sulfurs. However the nonbonding Li1--S2,3 and Li2--S2,3 distances are rather long, and such interactions, if any, would be very weak: Li1--S2, 3.23 Å; Li1--S3, 2.97 Å; Li2--S2, 3.02 Å; Li2--S3, 3.24 Å.

Crystal Structure of 4. Compound **4** crystallizes in the triclinic space group $P\bar{1}$, and the asymmetric unit contains a molecular unit of $Li_2Se_5(pmdeta)_2$. Figure 4 shows a view of the molecular structure. Although there are no unusually strong intermolecular interactions in the lattice, somewhat short contacts occur between Se5 and Li2′ (x, $1-y$, $1-z$), between Se5 and a neighboring Se5′ atom (x, $1-y$, $1-z$), and between C11 and C18′ ($-1-x$, $1-y$, $1-z$), with the separations being 3.07(1), 3.353(2), and 3.39(1) Å, respectively. Table VII presents selected intramolecular bond distances and bond angles.

The X-ray analysis unambiguously demonstrates that the Li_2Se_2/pmdeta system in toluene gives rise to a pentaselenide. This

(14) Amstutz, R.; Seebach, D.; Seiler, P.; Achweizer, B.; Dunitz, J. D. *Angew. Chem., Int. Ed. Engl.* **1980**, *19*, 53.
(15) (a) Tatsumi, K.; Inoue, Y.; Nakamura, A.; Cramer, R. E.; VanDoorne, W.; Gilje, J. W. *J. Am. Chem. Soc.* **1989**, *111*, 782. (b) Tatsumi, K.; Inoue, Y.; Kawaguchi, H.; Kohsaka, M.; Nakamura, A.; Cramer, R. E.; VanDoorne, W.; Taogoshi, G. J.; Richmann, P. N. *Organometallics* **1993**, *12*, 352.
(16) Tatsumi, K.; Matsubara, I.; Inoue, Y.; Nakamura, A.; Cramer, R. E.; Taogoshi, G. J.; Golen, J. A.; Gilje, J. W. *Inorg. Chem.* **1990**, *29*, 4928.
(17) Weiss, E.; Joergens, U. *Chem. Ber.* **1972**, *105*, 481.
(18) Gilardi, R.; Flippen-Anderson, J. L. *Acta Crystallogr., Sect. C* **1985**, *C41*, 72.
(19) Dubis, D.; Fackler, J. P., Jr. *Inorg. Chem.* **1982**, *21*, 3577.
(20) Coucouvanis, D.; Patil, P. R.; Kanatzidis, M. G.; Detering, B.; Baenziger, N. C. *Inorg. Chem.* **1985**, *24*, 24.

Table VII. Selected Bond Distances (Å) and Bond Angles (deg) for $Li_2Se_4(pmdeta)_2$ (**4**) with Esd's in Parentheses

Se1–Se2	2.307(2)	Li1–N1	2.04(2)
Se2–Se3	2.360(2)	Li1–N2	2.07(2)
Se3–Se4	2.330(1)	Li1–N3	2.12(2)
Se4–Se5	2.328(2)	Li2–N4	2.16(1)
Li1–Se1	2.56(1)	Li2–N5	2.16(1)
Li2–Se5	2.62(1)	Li2–N6	2.15(1)
Li1–Se1–Se2	100.4(3)	N1–Li1–N3	114.7(7)
Se1–Se2–Se3	108.05(6)	N2–Li1–N3	89.8(6)
Se2–Se3–Se4	109.89(5)	Se5–Li2–N4	112.9(5)
Se3–Se4–Se5	109.33(5)	Se5–Li2–N5	115.1(6)
Se4–Se5–Li2	117.7(3)	Se5–Li2–N6	117.3(6)
Se1–Li1–N1	120.2(7)	N4–Li2–N5	83.7(5)
Se1–Li1–N2	121.7(7)	N4–Li2–N6	128.9(6)
Se1–Li1–N3	115.4(6)	N5–Li2–N6	83.5(5)
N1–Li1–N2	88.5(6)		

contrasts with the formation of a tetrasulfide chain from the analogous Li_2S_2/pmdeta system in the same solvent. The reason for the different nuclearity is unknown. The two terminal Se atoms each coordinate to a lithium cation, to which a pmdeta ligand is also bonded. The mean Li–Se bond length of 2.59 Å compares well with the rare examples of known Li–Se bond lengths in $Cp^*Ta(Se)_3Li_3Cl(thf)_3$ (2.60 Å) and $Cp^*Ta(Se)_3Li_2(tmeda)_2$ (2.56 Å)[21] and is also close to the sum of the ionic radii of Li(I) and Se(–II) (2.57 Å).[22] Complex **4** is the first structurally characterized lithium polyselenide, while unligated Se_5^{2-} chains were found in the structures of $[Cs(18\text{-crown-}6)]_2Se_5$,[23] Cs_2Se_5,[24] and Rb_2Se_5.[25]

Having two lithiums strongly bound to the terminal Se atoms, the resulting seven-atom $LiSe_5Li$ skeleton forms a zigzag chain. The mean Se–Se–Se angle of 109.0° is normal, and it is also very similar to the S–S–S angles of **3**. An interesting geometrical difference between **3** and **4** can be seen in the Li–Se–Se angles of 100.4(3) and 117.7(3)°, which are substantially larger than the Li–S–S angles in **3**. The Li–Se–Se–Se torsional angles of 98.7 and 78.4° also contrast to the nearly-cisoid disposition of the Li–S–S–S frame in **3**, where the mean torsional angle is a small 23.9°.

The known Se_5^{2-} chains all have a shorter terminal Se–Se bond.[23-25] One of the terminal Se–Se bonds of **4** (Se1–Se2) is also shorter than the inner bonds. However, the Se4–Se5 bond is elongated by 0.02 Å compared to Se1–Se2 and is indistinguishable from Se3–Se4. The weak intermolecular contacts occurring between Li2 and Se5′ of the neighboring molecule (and *vice versa*) may be the cause of this elongation. As in the case of **3**, the N–Li–N angles associated with outer amine nitrogens of pmdeta are much larger than the other N–Li–N angles. While Li1 moves out of the N1–N3–Se1 plane by 0.40 Å toward N2, displacement of Li2 from the N4–N6–Se5 plane is only 0.12 Å, opening up one side of the Li coordination sphere. This open site is where the Li2--Se5′ (and Li2′--Se5) intermolecular contact takes place.

Raman Spectra of the Polysulfides. The upper part of Figure 5 superimposes the Raman spectra for crystalline samples of **1**–**3**. The spectrum of S_8 is also displayed at the bottom of Figure 5 for comparison. It is evident that the structurally similar complexes, **1** and **2**, exhibit nearly identical spectral patterns, while that of **3** differs.

Raman studies of known polysulfide chains of alkali and alkaline-earth complexes have demonstrated that the bands arising from S–S stretching vibrations appear in the 350–500-cm^{-1} region.[26] For instance, two intense bands at 434 and 486 cm^{-1} were observed for polycrystalline samples of K_2S_4, which were assigned to two S–S symmetric stretching fundamentals. For Na_2S_4, the corresponding bands come at 445 and 482 cm^{-1}.

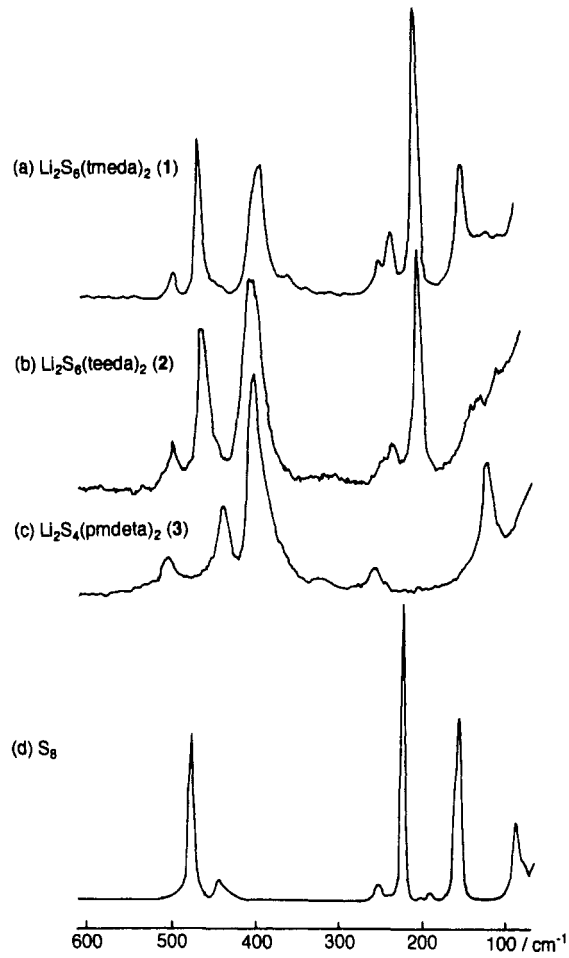

Figure 5. Comparison of the Raman spectra in the 100–600-cm^{-1} region for crystalline samples of **1**–**3**. The spectrum of S_8 (powder) is also superimposed.

The Raman spectrum of **3** indeed exhibits intense bands at 402 and 440 cm^{-1} and a relatively weaker band at 505 cm^{-1}. By reference to the spectra of K_2S_4 and Na_2S_4, the two bands at higher frequencies may be attributed to symmetric S–S stretches. If this assignment is correct, then the 402-cm^{-1} band could originate from the Li-bound pmdeta ligand, although metal-free pmdeta does not show Raman bands in this region. However, it is also possible that the 402-cm^{-1} band arises from S_4^{2-} skeletal vibrations because the stretching vibrational modes may be perturbed by the strong lithium–sulfur interactions.

The Raman spectra of **1** and **2** show bands at 395, 471, and 500 cm^{-1} and at 405, 466, and 498 cm^{-1}, respectively, which correspond to the three bands described above for **3**. Again, it is not clear whether the 395-cm^{-1} band derives from the S_6^{2-} skeleton or from the Li-bound tmeda (or teeda) ligand. An interesting aspect of the spectra of **1** and **2** is that they have an intense band at 205 cm^{-1} (**1**) or 204 cm^{-1} (**2**). In the case of **1**, an additional line appears at 148 cm^{-1}, while for **2** the quality of the spectrum in this region is insufficient for interpretation. These

(21) Tatsumi, K.; Kawaguchi, H.; Tani, K. *Angew. Chem., Int. Ed. Engl.* **1993**, *32*, 591.
(22) Shannon, R. D. *Acta Crystallogr., Sect. A* **1976**, *A32*, 751.
(23) Brese, N. E.; Randall, C. R.; Ibers, J. A. *Inorg. Chem.* **1988**, *27*, 940.
(24) Kretschmann, U.; Böttcher, P. *Z. Naturforsch., B: Anorg. Chem., Org. Chem.* **1985**, *40B*, 895.
(25) Böttcher, P. *Z. Krystallogr.* **1979**, *150*, 65.
(26) (a) Eysel, H. H.; Wieghardt, G.; Kleinschmager, H.; Weddingen, Z. *Naturforsch., B: Anorg. Chem., Org. Chem.* **1976**, *31B*, 415. (b) Daly, F. P.; Brown, C. W. E. *J. Phys. Chem.* **1975**, *79*, 350. (c) Janz, G. J.; Roduner, E.; Coutts, J. W.; Downey, J. R., Jr. *Inorg. Chem.* **1976**, *15*, 1751. (d) Janz, G. J.; Coutts, J. W.; Downey, J. R., Jr.; Roduner, E. *Inorg. Chem.* **1976**, *15*, 1755. (e) Janz, G. J.; Downey, J. R., Jr.; Roduner, E.; Wasilczyk, G. J.; Coutts, J. W.; Eluard, A. *Inorg. Chem.* **1976**, *15*, 1759. (f) Steudel, R. *J. Phys. Chem.* **1976**, *80*, 1516. (g) Ziemann, H.; Bues, W. *Z. Anorg. Allg. Chem.* **1979**, *455*, 69.

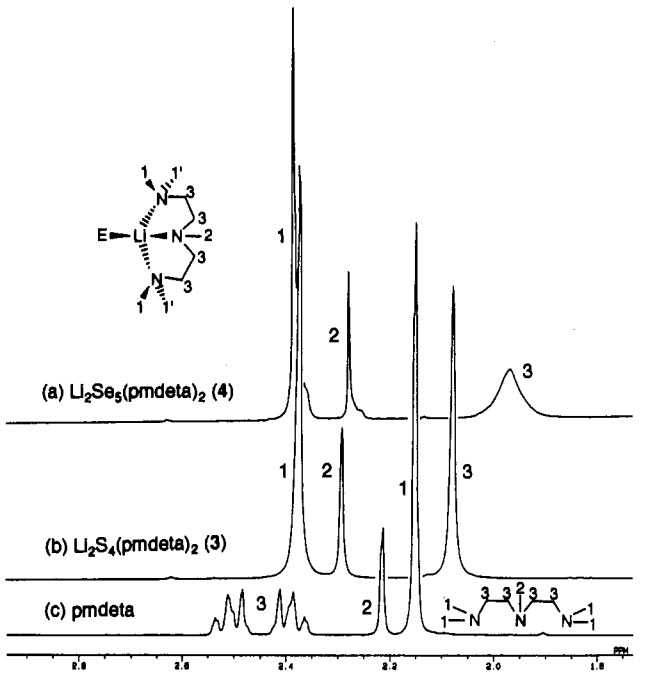

Figure 6. Comparison of the 270-MHz ^1H NMR spectra of **3**, **4**, and pmdeta.

low-frequency Raman lines are unlikely to arise from the Li-bound amines and seem to be associated with the bicyclic Li_2S_6 arrangement. Supporting this interpretation are the intense lines at 218 and 152 cm^{-1} in the S_8 (powder) spectra. These two low-frequency S_8 bands were assigned to e_1 and e_2 bending modes characteristic of the cyclic S_8 geometry,[27] and we think the corresponding bands for **1** and **2** are of a similar origin.

^1H NMR Spectra. The room-temperature ^1H NMR spectra of **2**–**5** in C_6D_6 deserve comment. The spectrum of **2** features a group of teeda signals, a quartet at 2.66 ppm arising from the methylene protons of the ethyl group, a singlet at 2.36 ppm from the ethylene protons, and a triplet at 1.02 ppm from the methyl protons of the ethyl group. The corresponding peaks for free teeda come at 2.53 ppm (quartet), 2.61 ppm (singlet), and 1.06 ppm (triplet). Thus in the order from free teeda to **2**, the quartet shifts downfield, while the singlet moves to upfield. As a consequence, the relative positioning of these teeda resonances are inverted upon teeda coordination to lithium.

Likewise, we observed reversal of the methyl (2.18 ppm) and ethylene (2.00 ppm) signals of tmeda in **1**, where those resonances for free tmeda are at 2.26 ppm (methyl) and 2.39 ppm (ethylene). The appearance of a single set of teeda (and tmeda) signals for **2** (and for **1**), which are clearly shifted from those of the free ligands, indicates that Li–diamine interactions remain strong in a C_6D_6 solution and that dissociation, if it occurs, is slight.

The pmdeta signals of **3** at room temperature are compared with those of the free ligand in Figure 6. The A_2B_2 multiplet of ethylene protons of free pmdeta moves upfield and becomes a singlet for **3**, while the peak arising from the terminal methyl protons is shifted downfield. According to a variable-temperature NMR study in toluene-d_8, the signals of the terminal methyl protons and the ethylene protons broaden as the temperature is lowered and the former coalesces at ca. −90 °C, during which time the inner methyl signal remains sharp. Thus, equilibration of the terminal methyl groups in solution is stopped at low temperatures. Unfortunately, it is not possible to comment on whether the four methyl groups are all nonequivalent or are grouped into two sets, because we are unable to reach the slow-exchange limit. However, these observations point to the presence of strong interactions between pmdeta and lithium in C_6D_6 and toluene-d_8 solutions.

The principal feature of the room-temperature ^1H NMR spectra observed for the lithium polysulfides is carried over to the polyselenide complexes. The tmeda adduct of lithium selenide (**5**) gives a spectrum in which the methyl signal (2.26 ppm) again comes at a lower field than the ethylene signal (1.95 ppm). Also the spectrum of $Li_2Se_5(pmdeta)_2$ (**4**), shown at the top of Figure 6, is not much different from the one observed for **3**, except that the resonance of the ethylene protons is broader. Pmdeta in **4** may be less mobile.

(27) (a) Scott, D. W.; McCullough, J. P. *J. Mol. Spectrosc.* **1964**, *13*, 313. (b) Steudel, R.; Mäusle, H.-J. *Z. Naturforsch., A: Phys. Chem., Kosmophys.* **1978**, *33A*, 951.

Supplementary Material Available: Tables of crystal data, positional and thermal parameters, and bond distances and angles for **2**, **3**, and **4** (19 pages). Ordering information is given on any current masthead page.